This article was downloaded by:
On: *25 January 2011*
Access details: *Access Details: Free Access*
Publisher *Taylor & Francis*
Informa Ltd Registered in England and Wales Registered Number: 1072954 Registered office: Mortimer House, 37-41 Mortimer Street, London W1T 3JH, UK

Liquid Crystals
Publication details, including instructions for authors and subscription information:
http://www.informaworld.com/smpp/title~content=t713926090

The synthesis and thermal, optical and electrical properties of novel aromatic-aliphatic five- and six-membered thermotropic polyimides

Ewa Schab-Balcerzak[ab]; Marcin Wegrzyn[a]; Henryk Janeczek[a]; Bozena Jarzabek[a]; Patrice Rannou[c]; Agnieszka Iwan[d]
[a] Centre of Polymer and Carbon Materials, Polish Academy of Sciences, Zabrze, Poland [b] Institute of Chemistry, University of Silesia, Katowice, Poland [c] Laboratoire d'Electronique Moléculaire, Organique et Hybride, Institut Nanosciences & Cryogénie, CEA-Grenoble, Grenoble Cedex 9, France [d] Electrotechnical Institute, Division of Electrotechnology and Materials Science, Wroclaw, Poland

Online publication date: 15 November 2010

To cite this Article Schab-Balcerzak, Ewa , Wegrzyn, Marcin , Janeczek, Henryk , Jarzabek, Bozena , Rannou, Patrice and Iwan, Agnieszka(2010) 'The synthesis and thermal, optical and electrical properties of novel aromatic-aliphatic five- and six-membered thermotropic polyimides', Liquid Crystals, 37: 11, 1347 — 1359
To link to this Article: DOI: 10.1080/02678292.2010.506578
URL: http://dx.doi.org/10.1080/02678292.2010.506578

PLEASE SCROLL DOWN FOR ARTICLE

Full terms and conditions of use: http://www.informaworld.com/terms-and-conditions-of-access.pdf

This article may be used for research, teaching and private study purposes. Any substantial or systematic reproduction, re-distribution, re-selling, loan or sub-licensing, systematic supply or distribution in any form to anyone is expressly forbidden.

The publisher does not give any warranty express or implied or make any representation that the contents will be complete or accurate or up to date. The accuracy of any instructions, formulae and drug doses should be independently verified with primary sources. The publisher shall not be liable for any loss, actions, claims, proceedings, demand or costs or damages whatsoever or howsoever caused arising directly or indirectly in connection with or arising out of the use of this material.

Liquid Crystals,
Vol. 37, No. 11, November 2010, 1347–1359

Taylor & Francis
Taylor & Francis Group

The synthesis and thermal, optical and electrical properties of novel aromatic–aliphatic five- and six-membered thermotropic polyimides

Ewa Schab-Balcerzak[a,b]*, Marcin Wegrzyn[a], Henryk Janeczek[a], Bozena Jarzabek[a], Patrice Rannou[c] and Agnieszka Iwan[d]*

[a]*Centre of Polymer and Carbon Materials, Polish Academy of Sciences, Zabrze, Poland;* [b]*Institute of Chemistry, University of Silesia, Katowice, Poland;* [c]*Laboratoire d'Electronique Moléculaire, Organique et Hybride, Institut Nanosciences & Cryogénie, CEA–Grenoble, Grenoble Cedex 9, France;* [d]*Electrotechnical Institute, Division of Electrotechnology and Materials Science, Wroclaw, Poland*

(*Received 16 March 2010; final version received 2 July 2010*)

Polymers have been prepared by the polycondensation of 4,4′-(butane-1,4-diylbis(oxy)) bis(butane-4,1-diyl) bis(4-aminobenzoate) and 5,10,15,20,25,30,35,40,45,50,55,60-dodecaoxatetrahexacontane-1,64-diyl bis(4-aminobenzoate) (PBBA 1200) with three dianhydrides based on naphthalene, perylene and phthalic moieties, respectively. This has resulted in five novel aliphatic–aromatic polyimides. The polyimides differed in aliphatic chain length and whether the imide ring was five- or six-membered. The chemical structure of the polyimides has been confirmed by ^{1}H NMR and FTIR spectroscopy and by elemental analysis. The optical and electrical properties of the polyimides have been studied using current–voltage measurements, and the effect of the polyimide structure on thermal and mesomorphic behaviour investigated by differential scanning calorimetry and polarising optical microscopy. Wide-angle X-ray diffraction at different temperatures was employed to confirm the structural properties of the polyimides. All the novel polyimides, with the sole exception of that obtained from PBBA1200 and 3,4,9,10-perylenetetracarboxylic dianhydride, showed liquid crystalline properties. As far as we are aware, this is the first time that six-membered polyimides exhibiting liquid crystalline properties have been reported.

Keywords: polyimide; polynaphthimide; perylene moieties; thermotropic liquid crystals

Downloaded At: 13:42 25 January 2011

1. Introduction

Polyimides play a key role in a number of applications, ranging from dielectric films for the electronic industry and orientation layers liquid crystal industry, lightweight load-bearing heat-resistant composites and adhesives for the aerospace industry, to gas-separation membranes. Their importance arises from their chemical resistance and their outstanding thermal, mechanical and electrical properties [1, 2].

The polyimides investigated can be divided into those containing either five-membered or six-membered imide rings. Among the varieties of polyimides investigated, those with six-membered imide rings, obtained from naphthalene tetracarboxylic dianhydride (NTDA) and perylene tetracarboxylic dianhydride (PTDA), were particularly interesting. Perylene and naphthalene diimides are important due to their photochemical behaviour, excellent thermal and photo-stability and their photo-conductive properties [3–5]. Recently they have received attention due to their tendency to form n-type organic semiconductors [6–9].

Both the five- and the six-membered aromatic imide groups are almost planar, and are also rigid, polar and thermostable. They are therefore promising as components of liquid crystalline (LC) polymers, regardless of their thermotropic or lyotropic character [10]. Thermotropic liquid crystals (TLC) possess a number of unique properties and have received considerable attention, and significant efforts have been focused on the synthesis of new compounds [11, 12]. Polyimides are widely used in LC alignment layers to induce uniform unidirectional alignment, which is critical to the optical and electrical performance of industrial LC flat-panel display devices [13, 14]. In addition, polyimides may themselves exhibit liquid crystalline properties, and among the TLC polymers previously studied a variety of five-membered LC polyimides have been examined [10, 15–23]. An example is a LC copoly(amide-imide) synthesised from pyromellitic dianhydride, terephthaloyl chloride and 1,3-bis[4-(4′-aminophenoxy)cumyl]benzene, which transforms from smectic C to smectic A phase [19]. A LC polyimide has also been obtained from 4,4′-terphenyltetracarboxylic acid and 1,11-diaminoundecane [20].

A series of poly(ester-imide)s has been found to show mesomorphism [12, 13, 18]. Typical examples of

*Corresponding author. Email: eschab-balcerzak@cmpw-pan.edu.pl; ewa.schab-balcerzak@us.edu.pl; a.iwan@iel.wroc.pl

ISSN 0267-8292 print/ISSN 1366-5855 online
© 2010 Taylor & Francis
DOI: 10.1080/02678292.2010.506578
http://www.informaworld.com

LC poly(ester-imide)s have been obtained from 1,4-bis[4-(4-aminophenoxy)phenoxy]benzene and 3,3′, 4,4′-biphenyltetracarboxylic dianhydride (BPDA) and these show nematic and smectic A mesophases. BPDA has similarly been used in reactions with α,ω-bis (4-aminophenoxy)alkanes, with five or six ethylene oxide units as spacers. Transition temperatures for these compounds lie in the range 230–324°C when $n = 5$ and 235–300°C when $n = 6$. Most LC poly(ester imide)s containing cinnamoyl moieties and chiral groups exhibit mesomorphism up to 200°C with nematic, chiral nematic or Grandjean (blue) texture [22]. A series of copoly(ester imide)s synthesised by the esterification of *N,N′*-dodecane-1,12-diylbis(trimellitimide) with varying proportions of 4,4′-dihydroxybiphenyl and hydroquinone show enantiotropic smectic C phases [23].

The first example of an all-aromatic LC poly(ether imide), synthesised from BPDA and 1,4-bis[4-(4-aminophenoxy)phenoxy]benzene, is found to melt into a nematic phase [17]. Films prepared from this polymer by stretching the LC phase adopt the smectic A phase. A poly(siloxane imide) obtained from hydroquinone bis[(*N*-alkylphthalimide)-4-carboxylate] and 1,1,3,3-tetramethylsiloxane has shown a mesophase in the range 107–197°C [24].

On the other hand there have been few, if any, publications describing LC polyimides containing six-membered imide rings. Such polymers can be prepared from naphthalene dianhydrides, for example, 1,4,5,8-naphthalenetetracarboxylic dianhydride (NTDA) and 3,4,9,10-perylene tetracarboxylic dianhydride (PTDA). The naphthalene-1,4,5,8-tetracarboxylic imide unit is a highly symmetric mesogen and its L/D ratio is lower than those of typical short mesogens [25]. Kricheldorf has obtained polymers containing naphthalimide units, ester linkages and various lengths of aliphatic chain, but LC properties were not observed [25]. LC compounds containing perylene units have been investigated only as low molecular mass diimides, namely perylene diimides [26]. Generally speaking, the majority of publications relating to LC compounds based on naphthalene imide rings are equally related to diimides [7, 27].

It has been found that polymers containing perylene diimide or naphthalene diimide residues have potential applications in opto-electronic materials, including high efficiency solar cells and polarised light-emitting diodes [3, 28], and are particularly promising in photonic technology [29, 30]. It is important to combine the TLC and electrical properties of the polyimides to find practical applications for this group of polymers in LC semiconductors for producing electronics devices by the solution process.

The objective of the present work was to synthesise novel thermotropic five- and six-membered polyimides and study their photo-physical and (LC) properties. In this contribution we summarise the chemical (nuclear magnetic resonance (NMR) and Fourier transform infrared spectroscopy (FTIR)), thermal (differential scanning calorimetry (DSC) and thermo-gravimetric analysis (TGA), polarising optical microscopy (POM), X-ray (T)), optical (UV–Vis absorption spectroscopy) and electrical (current–voltage, *I–V*) characterisation of new thermotropic calamitic LC polyimides, including the first published examples of LC polyimides based on a six-membered imide ring.

2. Experimental

2.1 Materials

All chemicals and reagents were used as received from Aldrich.

2.2 Synthesis of polyimides from 4,4′-(butane-1,4-diylbis(oxy))bis(butane-4,1-diyl) bis(4-aminobenzoate) (PBBA 470)

2.2.1 Polyimide P1A

Into a round-bottomed flask, PBBA 470 (0.472 g, 1 mmol), *N*-methylpyrrolidone (NMP; 1.6 ml) and 1,2-dichlorobenzene (0.4 ml) were charged. After the PBBA 470 had dissolved, 1,2,4,5-benzenetetracarboxylic dianhydride (pyromellitic dianhydride, PMDA; 0.218 g, 1 mmol) was added. The mixture was heated under an argon atmosphere at 170°C for 24 h and then cooled to room temperature. The resulting brown solid was filtered off and washed with acetone. After drying under vacuum at 50°C for 2 h, the polyimide was obtained in 81% yield.

^{1}H NMR (300 MHz, DMSO, TMS) [ppm] δ 8.36 (m, 8H, H_{Ar} [phenylene]); 8.11 (m, 4H, 2 × H_{Ar}–C(O)O); 7,70 (m, 4H, 4 × H_{Ar}–N); 4,34 (m, 4H, 2 × CH_2–C(O)O); 3.28–3.33 (m, 8H, 4 × CH_2–O); 1.53–2.20 (m, 12H, 3 × $(CH_2)_2$).
FTIR (KBr) [cm^{-1}] ν 2936–2798 (aliphatic C–H), 1786, 1724 (imide C=O stretch), 1584 (C=C stretch), 1399 (C–N stretch), 761 (imide ring deformation).
Calc. for $(C_{36}H_{34}N_2O_{10})_n$ (mol. wt. 654.66): C, 66.05; H, 5.23; N, 4.28. Found: C, 65.18; H, 5.63; N, 4.48.

2.2.2 Polyimide P2A

Into a round-bottomed flask, PBBA 470 (0.236 g, 0.5 mmol), *m*-cresol (2.1 ml) and triethanolamine (TEA;

Downloaded At: 13:42 25 January 2011

0.2 ml, 1.5 mmol) were charged. After the PBBA had dissolved, 1,4,5,8-naphthalenetetracarboxylic dianhydride (NTDA; 0.134 g, 0.5 mmol) and benzoic acid (0.01 g, 0.08 mmol) were added. The mixture was heated under an argon atmosphere at 80°C for 20 h, at 180°C for 5 h, and then cooled to room temperature. The resulting dark brown solution was poured into acetone (150 ml). The resulting solid was filtered off and washed with acetone. After drying under vacuum at 35°C for 3 h, the polyimide was obtained as a light brown solid in 75% yield.

^{1}H NMR (300 MHz, DMSO, TMS) [ppm] δ 8.68 (m, 4H, [naphthalene]); 8.11 (s, 4H, 2 × H_{Ar}–C(O)O); 7.61 (s, 4H, 4 × H_{Ar}–N); 4.36–4.38 (m, 4H, 2 × CH_2–C(O)O); 3.36–3.51 (m, 8H, 4 × CH_2–O); 1.55–1.82 (m, 12H, 3 × $(CH_2)_2$); FTIR (KBr) [cm^{-1}] ν 2937–2798 (aliphatic C–H), 1716, 1677 (imide C=O stretch), 1582 (C=C stretch), 1347 (C–N stretch), 768 (imide ring deformation).
Calc. for $(C_{40}H_{36}N_2O_{10})_n$ (mol. wt. 704.72): C, 68.17; H, 5.15; N, 3.98. Found: C, 66.72; H, 5.31; N, 3.71.

2.3 Synthesis of polyimides from 5,10,15,20,25,30,35,40,45,50,55,60-dodecaoxatetrahexacontane-1,64-diyl bis(4-aminobenzoate) (*PBBA 1200*)

2.3.1 Polyimide P1B

Into a round-bottomed flask, PBBA 1200 (0.596 g, 0.5 mmol), NMP (0.8 ml) and 1,2-dichlorobenzene (0.2 ml) were charged. After the PBBA 1200 had dissolved, PMDA (0.109 g, 0.5 mmol) was added. The mixture was heated under an argon atmosphere at 175°C for 23 h and then cooled to room temperature. The resulting solution was poured into acetone (100 ml) and the precipitate filtered off and washed with acetone. After drying under vacuum at 75°C for 1 h, the polyimide was obtained as a light brown solid in 93% yield.

^{1}H NMR (300 MHz, DMSO, TMS) [ppm] δ 8.37 (m, 8H, H_{Ar} [phenylene]); 8.12–8.14 (m, 4H, 2 × H_{Ar}–C(O)O); 7.69–7.72 (s, 4H, 4 × H_{Ar}–N); 4.36 (m, 4H, 2 × CH_2–C(O)O); 3.28–3.33 (m, 8H, 4 × CH_2–O); 1.89–2.50 (m, 52H, 13 × $(CH_2)_2$). FTIR (KBr) [cm^{-1}] ν 2927–2798 (aliphatic C–H), 1786, 1727 (imide C=O stretch), 1608 (C=C stretch), 1398 (C–N stretch), 721 (imide ring deformation).
Calc. for $(C_{76}H_{114}N_2O_{19})_n$ (mol. wt. 1359.72): C, 67.13; H, 8.45; N, 2.06. Found: C, 62.81; H, 8.24; N, 2.02; M_n = 6,740 g mol^{-1}, M_w = 19,440 g mol^{-1}, M_w/M_n = 2.9.

2.3.2 Polyimide P2B

Into a round-bottomed flask, PBBA 1200 (0.596 g, 0.5 mmol), *m*-cresol (2.1 ml) and TEA (0.2 ml, 1.5 mmol) were charged. After the PBBA 1200 had dissolved, NTDA (0.134 g, 0.5 mmol) and benzoic acid (0.01 g, 0.08 mmol) were added. The mixture was heated under an argon atmosphere at 80°C for 20 h, at 180°C for 5 h and then cooled to room temperature. The resulting dark brown solution was poured into acetone (150 ml). The resulting solid was filtered off and washed with acetone. After drying under vacuum at 35°C for 3 h polyimide PB2 was obtained as a light brown solid at 75% yield.

^{1}H NMR (300 MHz, DMSO, TMS) [ppm] δ 8.72 (m, 4H, [naphthalene]); 8.11 (s, 4H, 2 × H_{Ar}–C(O)O); 7.62 (s, 4H, 4 × H_{Ar}–N); 4.33–4.38 (m, 4H, 2 × CH_2–C(O)O); 3.34–3.46 (m, 8H, 4 × CH_2–O); 1.51–1.84 (m, 12H, 3 × $(CH_2)_2$); FTIR (KBr) [cm^{-1}] ν 2940–2797 (aliphatic C–H), 1713, 1675 (imide C=O stretch), 1582 (C=C stretch), 1343 (C–N stretch), 768 (imide ring deformation).
Calc. for $(C_{80}H_{116}N_2O_{19})_n$ (mol. wt. 1409.78): C, 68.16; H, 8.29; N, 1.99. Found: C, 66.75; H, 8.03; N, 1.94. M_n = 6,820 g mol^{-1}, M_w = 24,600 g mol^{-1}, M_w/M_n = 3.6.

2.3.3 Polyimide P3B

Into a round-bottomed flask were charged PBBA 1200 (0.596 g, 0.5 mmol) and pyridine (4 ml). After the PBBA 1200 had dissolved, PTDA (0.196 g, 0.5 mmol) was added. The mixture was heated under an argon atmosphere at 110°C for 24 h and then cooled to room temperature. The resulting solution was filtered and poured into acetone (100 ml), and the precipitate filtered off and washed with acetone. After drying under vacuum at 75°C for 2 h, polyimide P3B was obtained as a black solid at 60% yield.

^{1}H NMR (300 MHz, DMSO, TMS) [ppm] δ 8.62 (m, 4H, [perylene]); 7.62 (s, 4H, 2 × H_{Ar}–C(O)O); 7.26 (s, 4H, 4 × H_{Ar}–N); 4.25 (m, 4H, 2 × CH_2–C(O)O); 3.15 (m, 48H, 12 × CH_2–O); 1.13–2.01 (m, 52H, 13 × $(CH_2)_2$); FTIR (KBr) [cm^{-1}] ν 2936–2862 (aliphatic C–H), 1703, 1662 (imide C=O stretch), 1594, 1578 (C=C stretch), 1359 (C–N stretch), 809 (imide ring deformation).

2.4 Measurements

FTIR spectra were obtained on a BIO–RAD FTS 40 A spectrometer in transmission mode using KBr pellets.

Downloaded At: 13:42 25 January 2011

Proton nuclear magnetic resonance (^{1}H NMR) spectra were recorded on a Bruker AC 300 MHz spectrometer using dimethyl-d_6 sulphoxide (DMSO-d_6) as solvent.

UV–Vis absorption spectra were recorded in solution and the solid state from films cast on glass, using a Jasco V570 UV–V–NIR spectrometer.

DSC was conducted on a TA–DSC 2010 apparatus under a nitrogen atmosphere, using sealed aluminium pans. The heating/cooling rate was 0.5°C min^{-1} from –20°C to above the clearing point. The transition temperatures were noted at the endothermic and exothermic peaks.

Thermo-gravimetric analysis was carried out on a Q–1500 apparatus at a heating rate of 20°C min^{-1} over the range 20–820°C under a nitrogen atmosphere.

The textures of the LC phase were observed using a POM system, comprising a Leica DMLM microscope (2.5×, 5×, 10×, 20× and 50×), operating in both transmission and reflection modes, a LINKAM LTS350 (–196°C to +350°C) hot-plate with CI94 temperature controller, and a JVC Numeric 3–CCD KYF75 camera (resolution: 1360 × 1024).

Current–voltage measurements were performed on an indium tin oxide (ITO)/polymer/Alq_3/Al device. The polyimide NMP solution was spin-cast on to an ITO-covered glass substrate at room temperature. Residual solvent was removed by heating the film *in vacuo*. The Alq_3 layer was prepared on the compound film surface by vacuum deposition at a pressure of 2×10^{-4} Pa and the Al electrode was vacuum deposited at a similar pressure. The area of the diodes was 9 mm^2. Current–voltage characteristics were recorded on a Keithley 6715 electrometer.

Wide-angle X-ray diffraction (WAXD(T)) patterns were recorded using powder on a Pulveraceous Diffractometer Dron – 2. Co-radiation filtered by Fe was applied.

The weight-average molecular weight and molecular weight distribution (M_w/M_n) values of the polymers were determined by size-exclusion chromatography (SEC), using the diode array detector of a Hewlett–Packard 1100 Chemstation equipped with a 300 × 7.5 mm Polymer Labs PLgel Mixed D 5 μm 10^{-4} Å column, using tetrahydrofuran (THF) as eluent and standard polystyrene for calibration.

3. Results and discussion

In this study polyimides with five- and six-membered imide rings, respectively, were synthesised and characterised. The polymers also differed in the length of the aliphatic chain between the imide units.

3.1 Synthesis and characterisation

Novel polyimides were prepared by high solution temperature polycondensation of each of the three dianhydrides, PMDA, NTDA and PTDA, with flexible diamines containing ester and ether linkages and a long aliphatic chain. The synthetic pathways and the chemical structure of the polyimides synthesised in the present study are indicated in Figure 1.

It is well known that polyimides prepared from PTDA or NTDA have poor solubility in organic solvents, and this normally limits their applicability. However, as mentioned earlier, polyimides based on perylene and naphthalene are important due to their photochemical behaviour and their excellent thermal, optical and photo-conductive properties. Introduction of PBBA moieties increases the solubility and processability of the polyimides, and additionally introduces mesomorphic behaviour.

All the polyimides in the present study formed transparent films of good optical quality. Their structure was confirmed by elemental, FTIR and NMR analysis. Figure 2 illustrates a typical FTIR spectrum for the imide group, using polymer P2A as an example.

The structure of the polyimides synthesised was confirmed from the FTIR spectra by noting the disappearance of the anhydride C=O vibration bands at 1792 and 1767 cm^{-1} in PMDA, at 1780 and 1768 cm^{-1} in NTDA (cf. Figure 2(a)) and at 1774 and 1743 cm^{-1} in PTDA. In addition, the appearance of imide C=O stretching vibration bands at 1778 and 1724 cm^{-1} correspond to asymmetrical and symmetrical stretching, respectively, in the five-membered imide ring. Similarly, those at 1716 and 1677 cm^{-1} (1703 and 1662 cm^{-1} in P3B), correspond to asymmetrical and symmetrical stretch in the six-membered imide ring (cf. Figure 2(a)). All the polymers exhibited absorption bands in the region of 1360 cm^{-1} (C–N stretch) and 770 cm^{-1} (imide ring deformation), together with absorption bands in the range 2940–2797 cm^{-1} attributed to aliphatic groups.

A typical ^{1}H NMR spectrum for the polyimides in DMSO–d_6 is illustrated in Figure 2b. The naphthalic and perylene protons, as well as phthalic protons between imide rings, appear at the most downfield point as a singlet. The spectral data were in accordance with the formulae expected. SEC measurements on the polymers soluble in THF (P1B and P2B) provided weight average molecular weight (M_w) values of 19,440 g mol^{-1} for P1B and 24,600 g mol^{-1} for P2B.

Polymer solubility was qualitatively determined by dissolving of 0.05 g of the solid polymer in 1 ml of organic solvent at room temperature and at 50°C. Table 1 shows the solubility of the polyimides in a selection of organic solvents.

Downloaded At: 13:42 25 January 2011

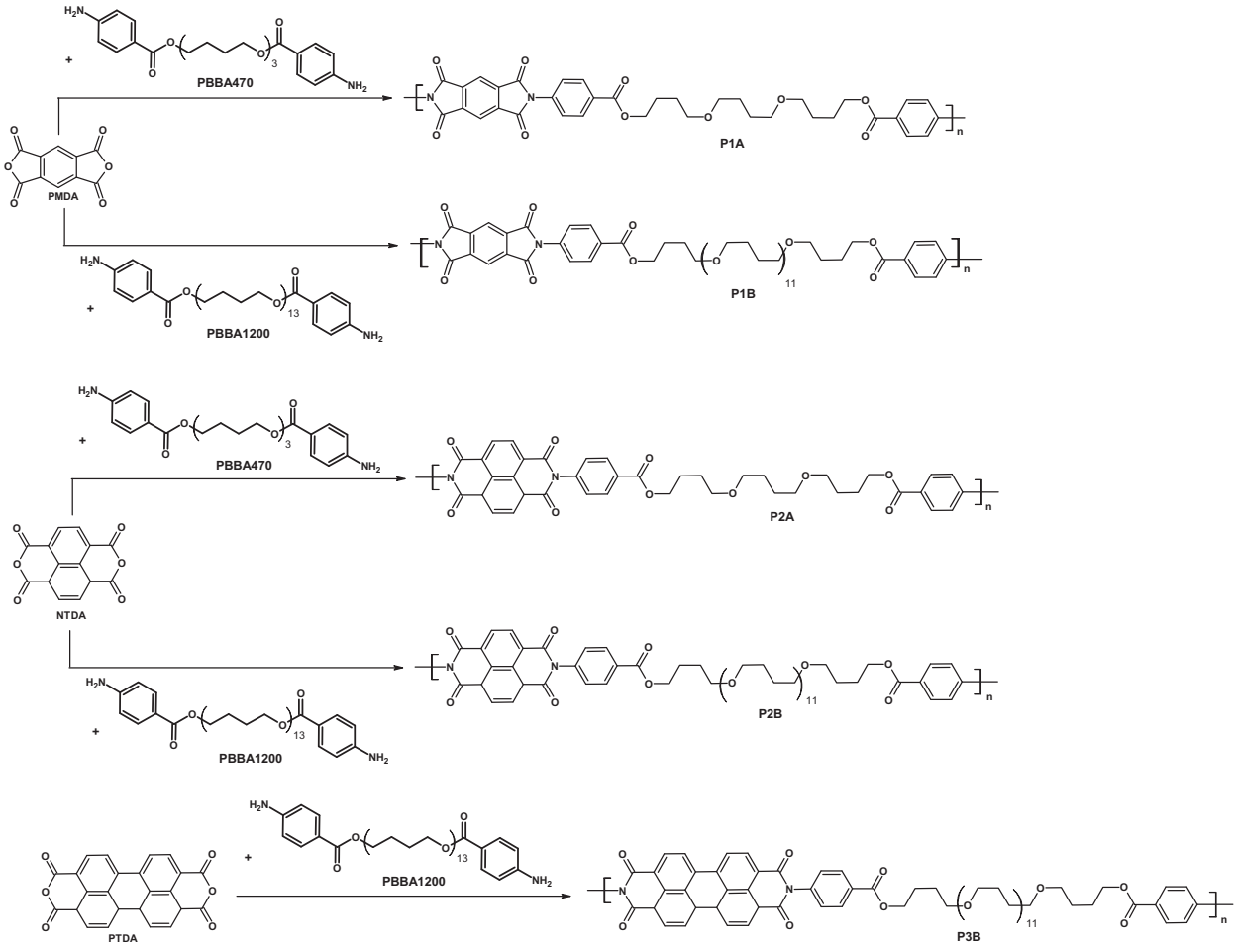

Figure 1. Synthetic route to the polyimides.

Downloaded At: 13:42 25 January 2011

It is seen that the novel polyimides varied in solubility behaviour in different organic solvents. Most of them (apart from P1A and P3B) were readily soluble at room temperature in polar aprotic solvents such as NMP. The solubility increases with temperature, and the polyimides (expect P1A) were soluble or partially soluble even in low-boiling ether-type solvents such as THF. Comparing the influence of the chemical constitution of the polymer backbone on the solubility it is concluded that polyimides obtained from PBBA 1200 exhibited better solubility than those derived from diamines with a shorter alkoxy chain, such as PBBA 470. It was found that polyimide P2B, synthesised from NTDA and PBBA 1200, exhibited higher solubility than the others. On the other hand P1A, derived from PMDA and PBBA 470 had poor solubility.

3.2 Optical properties

Electronic spectra of the polyimides were determined, both in solution and in the solid state as thin films cast on a glass substrate. The range of UV–Vis measurements was limited by the transparency of the solvent and the substrate. The results of the optical absorption measurements of the polyimides are summarised in Table 2.

Absorption properties in the UV–Vis range of all polymers were investigated in solution in NMP at a concentration of 10^{-5} mol l^{-1}. The absorption spectra of the polymers P1B, P2B and P3B in NMP solution are illustrated in Figure 3(a).

Polymer P2B showed two strong absorption peaks at 361 and 381 nm and a hump at 345 nm. A similarly shaped UV–Vis spectrum was observed with P3B, but in this case the bands showed a red-shift of more than 100 nm compared with P2B (see Figure 3(a) and Table 2). Polymer P1B, on the other hand, showed only one strong absorption peak, at 280 nm. These observations clearly demonstrate the influence of the dianhydride structure on the optical absorption characteristics of the polyimides. On the other hand, the diamine structure did not appear to influence the position of the absorption bands, confirming that

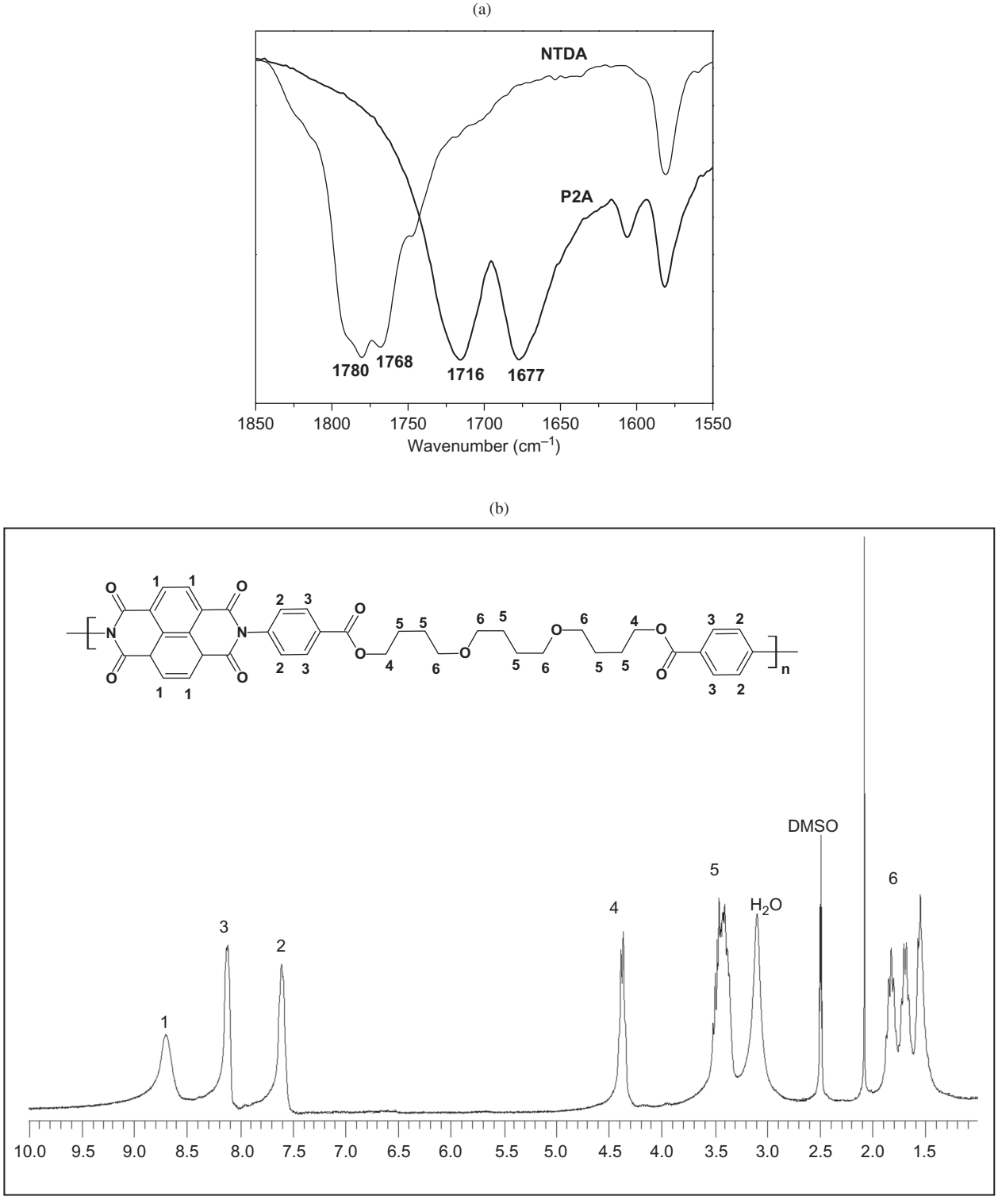

Figure 2. (a) FTIR and (b) ^{1}H NMR spectra of P2A (the FTIR spectrum of the dianhydride, NTDA, is included for comparison).

the optical properties of the polyimides were mainly influenced by the structure of the dianhydride.

Additionally, the solvatochromism of one typical polyimide, P2B, was evaluated by UV–Vis absorption spectroscopy. This was carried out in three different solvents, NMP, pyridine and *m*-cresol, and the results are presented in Figure 3(b). It will be seen that in NMP or pyridine, P2B does not exhibit

Downloaded At: 13:42 25 January 2011

Table 1. Solubility of the polymers.

Polyimide	Solvent						
	NMP	DMSO	*m*-cresol	pyridine	THF	CP	NB
P1A	–	±	++	–	–	+	±
P1B	+	±	++	++	++	++	++
P2A	+	++	+	++	±	+	++
P2B	+	++	+	+	++	+	+
P3B	±	±	±	±	±	±	±

Notes: Solubility was tested qualitatively on 0.05 g samples in 1 ml solvent: + indicates soluble at room temperature, ++ soluble on heating, ± partially soluble on heating, and – insoluble on heating. DMF: *N,N*-dimethylformamide; DMSO: dimethylsulphoxide; THF: tetrahydrofuran; CP: *p*-chlorophenol; NB: nitrobenzene.

solvatochromism. The UV–Vis spectrum of this polyimide in a protic solvent such as *m*-cresol demonstrated how the solvent can influence the shape of the absorption maximum band, in this case resulting from interaction between the hydrogen atom in the hydroxyl group of *m*-cresol and the polyimide chain. The changes in optical absorption spectra when the solvent was varied may be attributed to modification of the planarity of the polymer chain.

The absorption spectra of the polymers in solution were compared with those obtained from film (Table 2). UV–Vis absorption bands obtained from thin polymer films cast from NMP showed a red-shift in comparison with those from NMP solution. This seems to indicate that the chain conformation is different in solution and in films cast from the same solvent. This probably occurs when the transition dipole moments of the molecules are perpendicular, leading to the formation of so-called J-aggregates, and characterised by a bathochromic shift of bands in the UV–Vis absorption spectra.

In addition, the influence of solvent type on the UV–Vis absorption properties of the polyimides was investigated, and the results are also shown in Table 2. Figure 4 presents UV–Vis spectra of polyimides P2B and P3B cast on glass slides from different solvents.

No significant difference could be observed in the position or shape of the absorption bands in polyimide films cast from a variety of solvents.

3.3 Thermal properties

The thermal stability of polymers P1A, P1B and P2B was evaluated by thermo-gravimetric analysis (TGA) under a nitrogen atmosphere. The results are summarised in Table 3.

It is clear that the thermal properties of the polyimides depended strongly on their structure, in this case on the microstructure of the polymer backbone. Taking into account the chemical constitution of the polyimides used in the present study, one might expect that they should exhibit relatively poor thermal stability due to the long aliphatic elements in the repeat unit. However, the data presented in Table 3 show that these polymers exhibited good thermal stability. The initial decomposition (T_d) (based on 5% weight loss) and the temperature at which 10% weight loss occurred ($T_{10\%}$), which is usually considered the criterion for assessing the thermal stability of high-temperature polymers, lay within the range 360–390°C and 390–410°C, respectively. The polymer (P1A) obtained from PBBA470 began to decompose at a lower temperature than the polymer (P1B) from PBBA1200. However, in terms of carbonised residue, the percentage char yield at 800°C was higher for polymer P1B than for P1A. The

Table 2. Absorption maxima (λ_{max}) of the polymers in NMP solution and of films cast on glass slides.

Polymer	λ_{max} [nm]/[eV]			
	In solution	Cast film		
	in NMP	from NMP	from CP	from *m*-cresol
P1A	274, 285, 308*/ 4.52, 4.35, 4.02	nm	341/3.64	340, 370/3.65, 3.35
P1B	275, 285/4.51, 4.35	306, 376/4.05, 3.30	nm	nm
P2A	345*, 361, 381/ 3.59, 3.43, 3.25	nm	nm	339*, 364, 378/ 3.66, 3.41, 3.28
P2B	345*, 361, 381/ 3.59, 3.43, 3.25	330, 341, 375, 395/ 3.76, 3.64, 3.31, 3.14	nm	346*, 363, 381/ 3.58, 3.41, 3.25
P3B	461*, 489, 524/ 2.69, 2.53, 2.37	nm	370, 378, 503, 558/ 3.35, 3.28, 2.46, 2.22	340*, 375, 502, 548/ 3.65, 3.31, 2.47, 2.26

Notes: *The position of the absorption band was calculated using the second derivative method: the minimum of the second derivative of the absorption corresponds to the absorption maximum.
CP: *p*-chlorophenol; nm: not measured.

Downloaded At: 13:42 25 January 2011

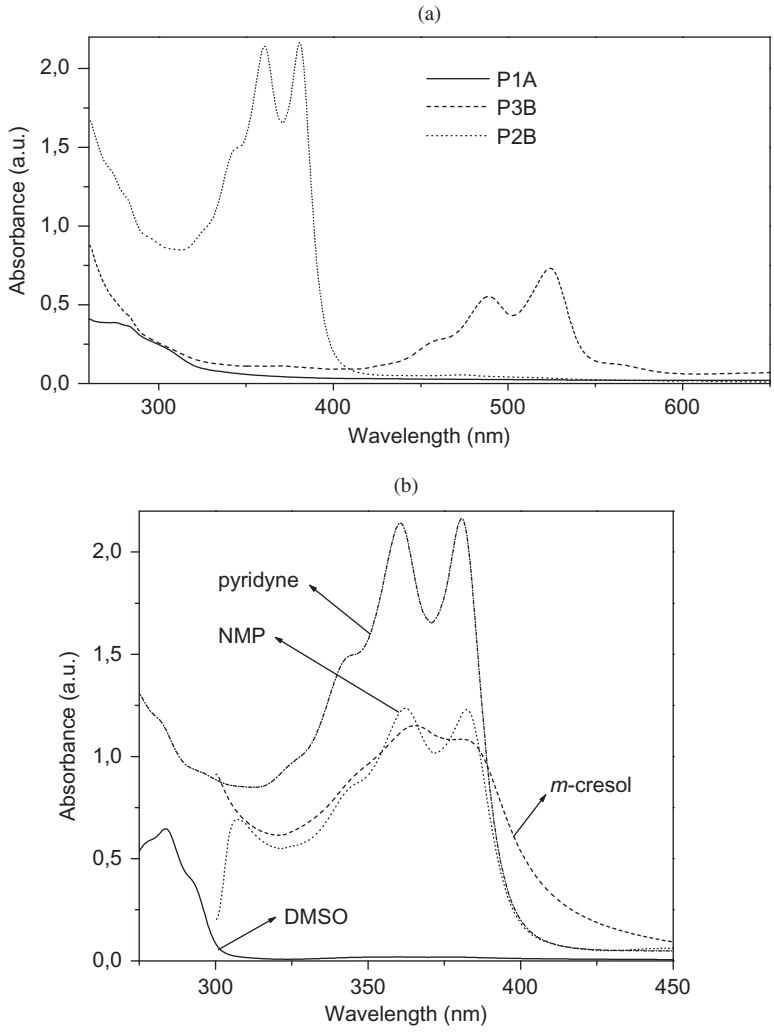

Figure 3. UV–Vis absorption spectra of (a) polyimides P2A, P3B and P1B in NMP solution, and (b) P2B in a range of solvents.

greatest percentage of residue at 800°C was exhibited by polymer P2B, which contained naphthalene units.

The main aim of introducing the PBBA structure into the polyimides was the possible generation of LC properties. The phase transitions and mesogenicity of the polyimides were studied by DSC and POM. All the DSC thermograms for the polyimides (apart from P3B) showed multiple melting peaks, indicating the presence of mesophases. Contrary to expectations, polymer P3B did not exhibit liquid crystalline properties. The DSC scans for P2A and P1A are shown in Figure 5.

P3B apart, it can be seen that DSC/POM analysis showed that the polyimides exhibited complex mesomorphic transitions, namely crystal-to-mesophase (Cr/M), mesophase–to–mesophase (M/M) and mesophase-to-isotropic (M/I). Details of the transition temperatures and associated enthalpy change of the polyimides determined by DSC are summarised in Table 4, and Table 5 identifies the phase variants of all the polyimides (other than P3B) determined by POM.

Tables 4 and 5 reveal that all the polyimides except P2B had clearing point temperatures above 270°C, and P2B had the lowest temperature of isotropisation. On the other hand, bearing in mind the length of the aliphatic region in the polyimides, we found that increasing rod length was accompanied by a decrease in the number of phase transitions, particularly in the case of P2A and P2B (Table 5).

It is also worth noting that the DSC measurements indicated an increase in melting temperature in the

Downloaded At: 13:42 25 January 2011

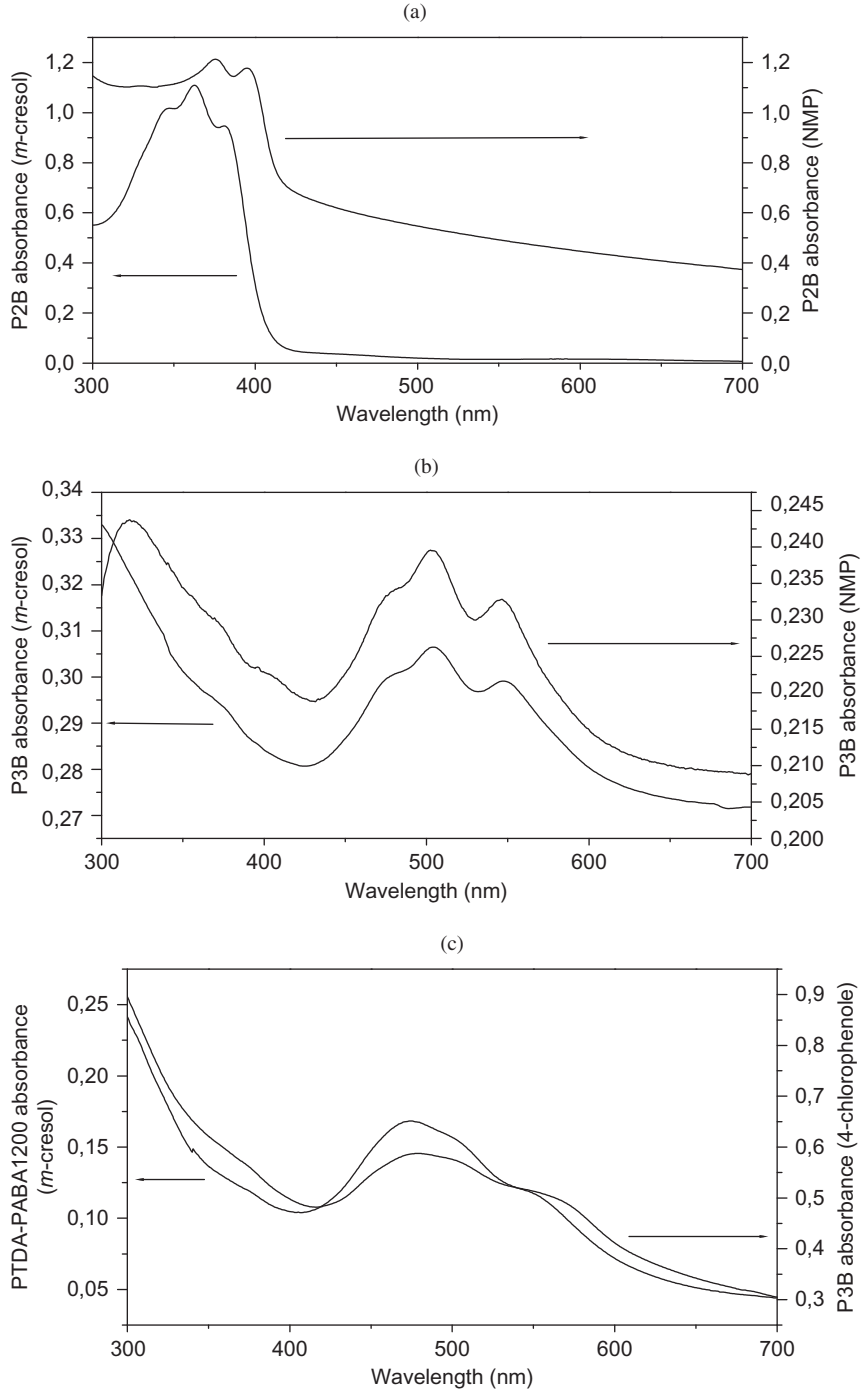

Figure 4. UV–Vis absorption spectra of polymer films (a) P2B and (b) P3B (each cast from *m*-cresol and NMP), and (c) P3B (cast from *m*-cresol and 4-chlorophenol).

order: P2A (123°C) < P1B (191°C) < P2B (205°C) < P1A (245°C). A similar sequence was observed in the melting temperatures of the polyimides from POM measurements (Table 5). The clearing temperatures were in a somewhat different sequence: P2B (230°C) < P1B (265°C) < P2A (270°C) < P1A (350°C) (Table 5).

The phase transitions were additionally analysed in terms of their enthalpy values. The melting process has the highest enthalpy values (Table 4). The enthalpy values decreased from 6.95 J mol^{-1} K for P2A to the minimal values 0.66 and 0.90 J mol^{-1} K for P2B and P1B, respectively.

Downloaded At: 13:42 25 January 2011

Table 3. Thermal properties of the polymers.

Polyimide	T_d (°C)	$T_{10\%}$ (°C)	$T_{15\%}$ (°C)	$T_{20\%}$ (°C)	$T_{30\%}$ (°C)	Residue at 800°C (%)
P1A	360	390	400	410	425	25
P1B	390	410	420	425	440	15
P2B	390	400	410	420	430	40

Notes: T_d: temperature at which 5% weight loss occurred.
$T_{10\%}$–$T_{30\%}$: Temperatures at which 10%–30% weight loss occurred.

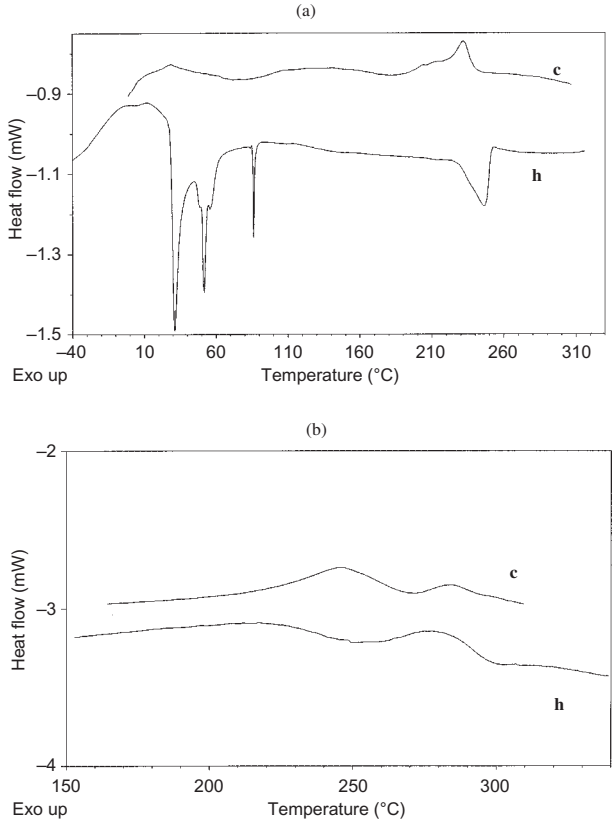

Figure 5. DSC scans for (a) P2A and (b) P1A during heating (h) and cooling (c).

Figure 6 shows microphotographs illustrating the texture of some of the polyimides studied.

Preliminary POM observations showed that the polyimides P1A, P1B and P2B exhibited one mesophase at high temperature (see Table 5). On cooling, P1A exhibited a broad LC phase in the range 330–250°C. Full isotropisation of P1A at about 350°C was observed and remained within a temperature range of about 20°C (Table 5). On the other hand, polymer P1B also showed one broad mesophase, in the range 245–175°C. Full isotropisation of P1B was observed at a lower temperature (about 260°C) than for P1A, and it too persisted over a temperature range of about 20°C (Table 5). The photomicrograph in

Table 4. Phase transition temperature of the polyimides detected by DSC (enthalpy values (ΔH) given in brackets).

Code	DSC (temperature, °C; ΔH, J g^{-1})
P1A	244.92 (4.96), 284.65 (1.56)
P1B	190.57 (3.42), 270.56 (0.90)
P2A	122.81 (4.77), 231.46 (6.95), 283.26 (1.44)
P2B	205.03, 217.73 (5.93), 235.91 (0.66)

Table 5. Thermal parameters of the polyimides determined by POM.

Code	Phase transitions detected on cooling, by POM (°C)
P1A	I ~ 350, M1 330, Cr 250
P1B	I > 265, M1 245, Cr 175
P2A	I > 270, M3 265, M2 242.5, M1 232.5, Cr 170
P2B	I 230, M1 215, M2 or Cr 205

Notes: M: mesophase; I: isotropisation; Cr: crystallisation.

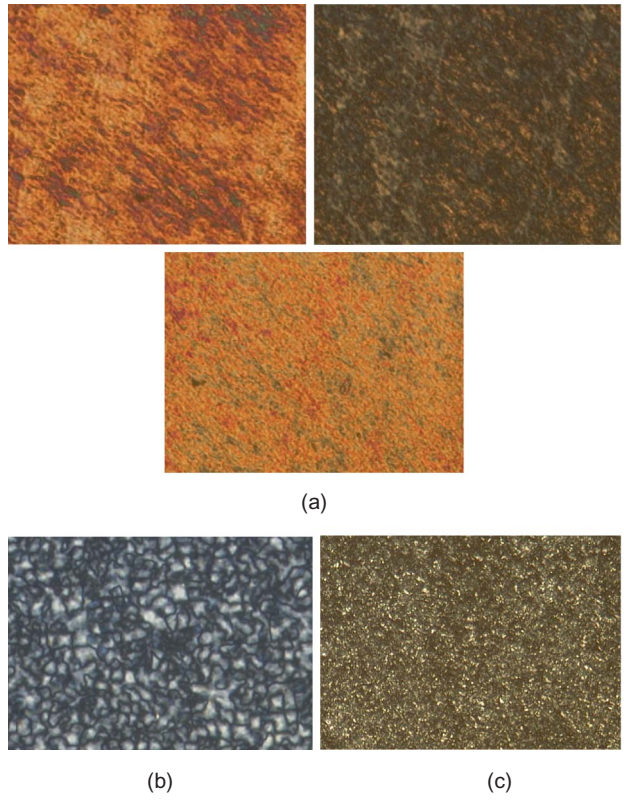

Figure 6. Photomicrographs showing the optical texture of mesophases obtained for (a) P2A (at 250, 240 and 220°C, respectively), (b) P2B (at 215°C) and (c) P1B (at 205°C) (colour version online).

Figure 6(c) shows the optical texture of the mesophase for P1B at 205°C.

It was curious that polymer P2B also exhibited one fairly narrow mesophase in the range 215–205°C. Full isotropisation of P2B was observed at a lower

Downloaded At: 13:42 25 January 2011

temperature (about 230°C) than in the case of P1B and existed over a temperature range of about 15°C (Table 5). The photomicrograph of the optical texture of the mesophase obtained for P2B at 215°C is given in Figure 6(b).

Rich polymorphism was found in P2A, the polyimide prepared from NTDA and PBBA 470. In the POM study P2A exhibited three quite narrow liquid crystal phases, M1, M2 and M3, in the range 265–170°C. Mesophase M1 was observed in the range 232–170°C (a 62°C temperature range), mesophase M2 occurred in the range 242–232 °C (a 10°C range), and mesophase M3 in the range 270–265°C (a range of 5°C) (Table 5). Full isotropisation of P2A was observed at about 270°C and existed over a temperature range of about 5°C. Photomicrographs of the optical textures of the mesophases obtained for P2A at 250, 240 and 220°C are presented in Figure 6(a).

POM measurements revealed textures which could indicate smectic (Sm) and/or nematic (N) mesophases. The SmA mesophase of P2B probably had a focal conic fan texture (Figure 6(b)). Identification of mesophases and the sequence of phase transitions were based on information provided by two references on liquid crystals [31, 32] and confirmed by repeat POM and DSC experiments.

3.4 Wide-angle X-ray diffraction (WAXD) studies

In order to investigate the structural changes occurring during the transitions detected by DSC measurements, X-ray diffractograms of the polymers were recorded at the temperature concerned, for example the temperature dependence of the X-ray solid-state diffraction patterns of P1B and P2A between values of 2θ of 8° and 45° are shown in Figure 7.

For polymer P1B the peaks at $2\theta = 22.27°$, 25.27°, 31.66° and 42.68° observed at 22°C shifted to lower values above 125°C. Additional heating from 125°C to 240°C generated diffraction peaks of higher intensity, at $2\theta = 21.54°$, 24.85°, 30.79° and 41.49°. The shift in the four diffraction peaks in P1B to lower values of 2θ could be ascribed to a crystallisation–mesophase transition. The WAXD observations were in good agreement with the POM results and confirmed the LC properties of P1B (Table 5). The X-ray diffraction profile in the lower 2θ region between 4° and 10° is shown in Figure 7; major shifts in the peaks with increasing temperature were not observed.

The temperature dependence of the X-ray solid state diffraction patterns in P2A is shown in Figure 7(b). At temperatures of 22°C and 100°C a broad diffraction halo was observed at $2\theta = 30.47°$. On heating from 100°C to 235°C, at 170°C two

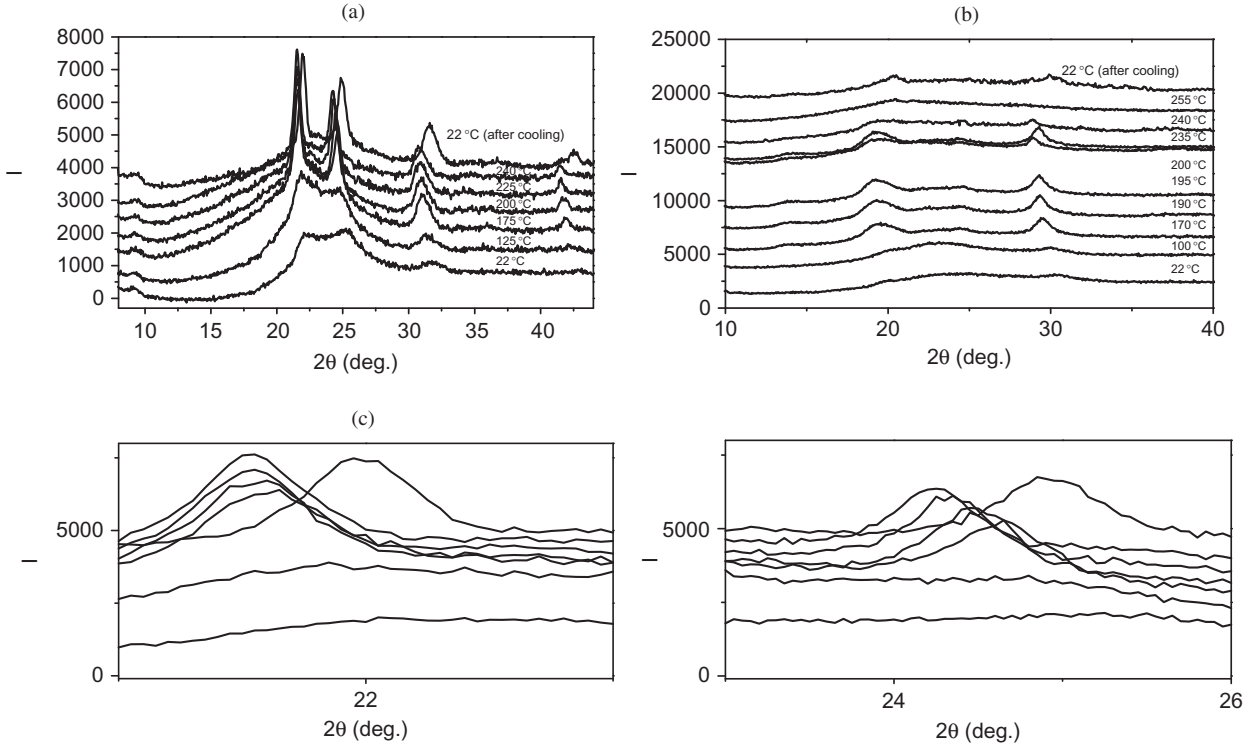

Figure 7. Temperature dependence of X–ray diffraction patterns of (a) P1B and (b) P2A between values of 2θ of 8 and 45°, and (c) X–ray diffraction patterns of P1B between values of 2θ of 20 and 23° (left-hand side) and between values of 2θ of 23 and 26° (right-hand side).

Downloaded At: 13:42 25 January 2011

peaks were observed, at $2\theta = 29.31°$ and 19.24°, and remained at 235°C. This X-ray behaviour confirmed the Cr–M1 transition of P2A (Table 5). Additional heating from 235°C to 255°C caused the diffraction peaks to disappear, which suggests that transition between mesophase M1 and mesophase M3 had taken place (Table 5).

All the diffraction peaks in the WAXD range of X-ray scattering are reversible during heating and cooling and disappeared in the same relatively narrow temperature range of the isotropisation transition of P2A; the same diffraction peaks reappeared simultaneously during cooling.

The scenario for the phase transitions in P1B (during a cooling scan: I > M1 > Cr), and in P2A (during a cooling scan: I > M3 > M2 > M1 > Cr) was thus fully confirmed, and supported by DSC, POM and WAXD.

3.5 *Current–voltage characteristics*

One type of sample architecture was used to demonstrate that the connection of organic and inorganic compounds improved the electrical properties of devices used as solar cells or organic light-emitting diodes (OLEDs). We fabricated a series of OLED devices with an Alq_3 green-emitting layer and an additional hole-transporting layer (HTL), comprising a thin film of polymer inserted between the ITO anode and the Alq_3 layer. (The abbreviation Alq_3 denotes tris(8-hydroxyquinolinato)aluminium, a compound with the formula $Al(C_9H_6NO)_3$. This is a coordination complex in which aluminium is bonded in a bidentate manner to the conjugate base of three 8-hydroxyquinoline ligands.)

I–V measurements were performed on an ITO/polymer/Alq_3/Al device. A schematic illustration of the device is presented in Figure 8(b). A solution in NMP was spin-cast on to an ITO-covered glass substrate at room temperature. *I–V* curves of ITO/polymer/Alq_3/Al are shown in Figure 8(a). It can be seen that the current increased with increase in the applied voltage.

As an example, at room temperature without illumination the turn-on voltage of the device ITO/P2A/Alq_3/Al was observed at about 7 V. On the other hand, the turn-on voltage of the device ITO/P3B/Alq_3/Al occurred at around 10 V at room temperature, and for the device ITO/P2B/Alq_3/Al without illumination it was found at about 13 V. The turn-on voltage of the device ITO/P1B/Alq_3/Al at room temperature was about 18 V.

This behaviour confirmed the influence of polymer structure on the *I–V* characteristics of the polyimides. The differences are caused by the change in planarity

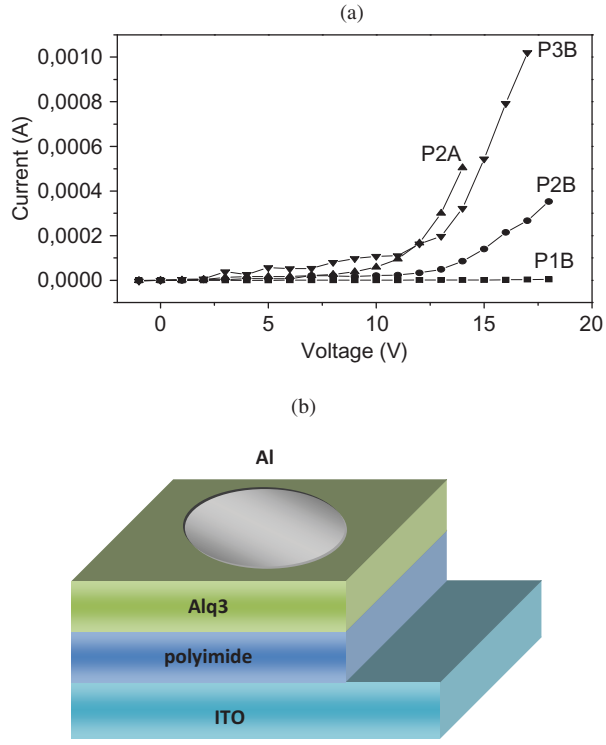

Figure 8. (a) Current–voltage curves of ITO/polymer/Alq_3/Al systems, and (b) a schematic diagram of the device used in the study.

in the structure of the polymers, and different conformations in film.

4. Conclusions

A novel series of thermotropic aromatic–aliphatic polyimides has been obtained by polycondensation of PBBA470 and PBBA1200 with each of three dianhydrides based respectively on naphthalene, perylene and phthalic moieties. Five new examples of aliphatic–aromatic polyimides have resulted and have been characterised by FTIR, NMR, DSC, POM, WAXD, UV–Vis and *I–V*. The conclusions to be drawn from the study are as follows:

- The polyimides exhibited good thermostability, with temperatures of initial decomposition within the range 360–390°C;
- The *I–V* characteristics of devices of the type ITO/polymer/Alq_3/Al confirmed the semiconducting nature of the polymer thin films; and
- All the polyimides other than P3B exhibited mesomorphic behaviour. Polymer P3B, which was based on perylene units, was exceptional and did not exhibit LC behaviour. Rich polymorphism was found in the case of P2A.

Downloaded At: 13:42 25 January 2011

This is believed to be the first time that thermotropic six-membered polyimides have been reported. The polyimides exhibited mesophases over a broad temperature range and could potentially be used in opto-electronic applications such as OLEDs and solar cells, by the use of imide-based HTLs, emissive layers, and electron-transporting layers (ETLs). Additionally, these polyimides could be used in mixtures with other LCs in displays.

Acknowledgements

The authors wish to thank Mr M. Domanski for his help in determining the *I–V* characteristics of the polyimides, and Dr W. Mielcarek for conducting the X-ray measurements. This research was partly carried out within the PAN/CNRS–DAE collaboration programme No. 22529.

References

[1] Ghosh, M.K., Mittal, K.L., Eds.; *Polyimides: Fundamentals and Applications*; Marcel Dekker, Inc.: New York, 1996.
[2] Hasegawa, M.; Horie, K. *Prog. Polym. Sci*. **2001**, *26*, 259–335.
[3] Jancy, B.; Asha, S.K. *J. Polym. Sci., Part A: Polym. Chem.* **2009**, *47*, 1224–1235.
[4] Nakazono, S.; Imazaki, Y.; Yoo, H.; Yang, J.; Sasamori, T.; Tokitoh, N.; Cedric, T.; Kageyama, H.; Kim, D.; Shinokubo, H.; Osuka, A. *Chem. Eur. J.* **2009**, *15*, 7530–7533.
[5] Bodapati, J.B.; Icil, H. *Dyes Pigm.* **2008**, *79*, 224–235.
[6] Bhosale, Sh.V.; Jani, Ch.H.; Langford, S.J. *Chem. Soc. Rev*. **2008**, *37*, 331–342.
[7] An, Z.; Yo, J.; Domercq, B.; Jones, S.C.; Barlow, S.; Kippelen, B.; Marder, S.R. *J. Mater. Chem.* **2009**, *19*, 6688–6698.
[8] Thelakkat, M.; Posh, P.; Schmidt, H.W. *Macromolecules* **2001**, *34*, 7441–7447.
[9] Jiang, W.; Tang, J.; Qi, Q.; Wu, W.; Sun, Y.; Fu, D. *Dyes Pigm.* **2009**, *81*, 11–16.
[10] Kricheldorf, H.R.; Linzer, V. *Polymer* **1995**, *36*, 1893–1902.
[11] Marin, L.; Damaceanu, M.D.; Timpu, D. *Soft Matter* **2009**, *7*, 1–20.
[12] Bhowmik, P.K.; Han, H.; Nedeltchev, A.K.; Mandal, H.D.; Jimenez-Hernandez, J.A.; McGannon, P.M.; Lopez, L.; Kang, Sh.-W.; Kumar, S. *Liq. Cryst.* **2009**, *36*, 1389–1399.
[13] Zhang, Q.; He, J.; Fang, Y.Q.; Wang, Y.-H. *Liq. Cryst.* **2008**, *35*, 385–388.
[14] Lai, H.; Liu, X.; Qin, L.; Li, M.; Gu, Y. *Liq. Cryst.* **2009**, *36*, 173–178.
[15] Kricheldorf, H.R. *Mol. Cryst. Liq. Cryst*. **1994**, *254*, 87–108.
[16] Orzeszko, A. *Macromol. Chem. Phys*. **1996**, *197*, 2461–2465.
[17] Dingemans, T.J.; Mendes, E.; Hinkley, J.J.; Weiser, E.S.; St Clair, T.L. *Macromolecules* **2008**, *41*, 2474–2483.
[18] Mourik, P.V.; Norder, B.; Mendes, E.; Picken, S.J.; Dingemans, T.J. *High Perform. Polym*. **2009**, *21*, 16–30.
[19] Liu, S.L.; Chung, T.S.; Geng, J.X.; Zhou, E.L.; Tamai, S. *Macromolecules* **2001**, *34*, 8710–8719.
[20] Inoue, T.; Kakimoto, M.; Imai, Y.; Watanabe, J. *Macromolecules* **1995**, *28*, 6368–6370.
[21] Kricheldorf, H.L.; Pakull, R. *Macromolecules* **1988**, *21*, 551–557.
[22] Sapich, B.; Stumpe, J.; Kircheldorf, H.R.; Fritz, A.; Schonhals, A. *Macromolecules* **2001**, *34*, 5694–5701.
[23] Leland, M.; Wu, Z.; Ho, R.-M.; Cheng, S.Z.D. *Macromolecules* **1998**, *31*, 22–29.
[24] Bialecka-Florjanczyk, E.; Orzeszko, A. *Polym. Bull*. **2002**, *48*, 431–438.
[25] Kricheldorf, H.R.; Jahnke, P. *Eur. Polym. J*. **1990**, *26*, 1009–1015.
[26] Struijk, C.W.; Sieval, A.B.; Dakhorst, J.E.J.; van Dijk, M.; Kimkes, P.; Koehorst, R.B.M.; Donker, H.; Schaafsma, T.J.; Picken, S.J.; van de Craats, A.M.; Warman, J.M.; Zulihof, H.; Sudholter, E.J.R. *J. Am. Chem. Soc.* **2000**, *122*, 11057–11066.
[27] Cormier, R.A.; Gregg, B.A. *Chem. Mater*. **1998**, *10*, 1309–1319.
[28] Wicklein, A.; Lang, A.; Muth, M.; Thelakkat, M. *J. Am. Chem. Soc*. **2009**, *131*, 14442–14453.
[29] Ofir, Y.; Zelichenok, A.; Yitzchaik, Sh. *J. Mater. Chem*. **2006**, *16*, 2142–2149.
[30] Yuney, K.; Icil, H. *Eur. Polym. J.* **2007**, *43*, 2308–2320.
[31] Gray, G.W.; Gooby, J.W. *Smectic Liquid Crystals: Textures and Structures*; Leonard Hill: Glasgow & London, 1984; pp 1–162.
[32] Tamaoki, N. *Adv. Mater.* **2001**, *13*, 1135–1147.

Downloaded At: 13:42 25 January 2011